

†Visitor from the U. S. Atomic Energy Commission.

¹These measurements were made during the initial period of low-intensity operation ($\sim 10^4$ muon stops/sec) and are the first muonic x-ray results to be reported from this facility.

²X. Campi, D. W. L. Sprung, and J. Martorell, Nucl. Phys. **A223**, 541 (1974).

³D. Vautherin, Phys. Rev. C **7**, 296 (1973).

⁴M. Brack, private communication.

⁵J. W. Negele and D. Vautherin, Phys. Rev. C **5**, 1472 (1972).

⁶T. Böhrringer, Travail de Diplôme, Eidgenössische Technische Hochschule Zürich, 1971 (unpublished).

⁷J. W. Negele, Nucl. Phys. **A142**, 225 (1970).

Neutral Currents in High-Energy Neutrino Collisions: An Experimental Search*

B. C. Barish, J. F. Bartlett, K. W. Brown, D. Buchholz, F. Jacquet,†
F. S. Merritt, F. J. Sciulli, and H. Suter‡
California Institute of Technology, Pasadena, California 91125

and

H. E. Fisk and G. Krafczyk
Fermi National Accelerator Laboratory, Batavia, Illinois 60510
(Received 23 December 1974)

A search for events with no final-state muon, as expected in the neutral-current interactions $\nu_\mu(\bar{\nu}_\mu) + N \rightarrow \nu_\mu(\bar{\nu}_\mu) + \text{hadrons}$, has been carried out by using the California Institute of Technology-Fermilab neutrino detector and narrow-band neutrino beam. A clear signal of events with no apparent final-state muon has been observed. Furthermore, missing energy in the final state for these events provides strong evidence for the existence of a final-state ν .

In recent years, theoretical developments¹ have implied that in addition to the familiar charged-current (CC) interactions

$$\nu_\mu(\bar{\nu}_\mu) + N \rightarrow \mu^-(\mu^+) + \text{hadron}, \quad (1)$$

there may exist neutral-current (NC) interactions

$$\nu_\mu(\bar{\nu}_\mu) + N \rightarrow \nu_\mu(\bar{\nu}_\mu) + \text{hadrons}. \quad (2)$$

Recent observations² of neutrino interactions without a visible final-state muon have been interpreted as examples of Reaction (2). The experiment described here was performed to search for such neutral-current phenomena.

The experiment used the Fermilab narrow-band neutrino beam,³ formed from a sign-selected hadron beam of 140 ± 30 GeV. The resulting neutrino spectrum consisted of two momentum bands centered at 45 and 125 GeV, plus a small wide-band component coming from decays before momentum selection. The target contained 143 tons of steel and measured $1.5 \text{ m} \times 1.5 \text{ m}$ in cross section and 14.2 m in length. It contained a calorimeter-detector consisting of seventy scintillation counters, spaced every 10 cm of steel (1 collision length), with a spark chamber after every second counter. The scintillation counters signaled the

passage of charged particles and measured the hadronic energy E_{had} by calorimetry.⁴ The spark chambers determined the transverse position of the interaction to ± 5 cm.

To collect a data sample unbiased by the presence or absence of a final-state muon, a special unrestricted trigger was constructed for this neutral-current search. It required only a measured hadronic energy deposition of ≥ 3 GeV and a minimal hadron-shower penetration of 2–4 collision lengths (CL) downstream of the interaction. To minimize cosmic-ray backgrounds fast-spill extraction from the accelerator ($\sim 400 \mu\text{sec}$) was used.

A set of simple criteria was applied to the data to obtain an uncontaminated and bias-free sample of events: (1) The two consecutive scintillation counters and the two spark chambers following the interaction indicated the presence of charged particles; (2) the interaction vertex was well within the steel target (at least 1.3 CL from the side, 4 CL from the front, and 14 CL from the downstream end); (3) a shower energy of $E_{\text{had}} \geq 6$ GeV was observed in the calorimeter. These requirements selected an almost pure sample of neutrino interactions.

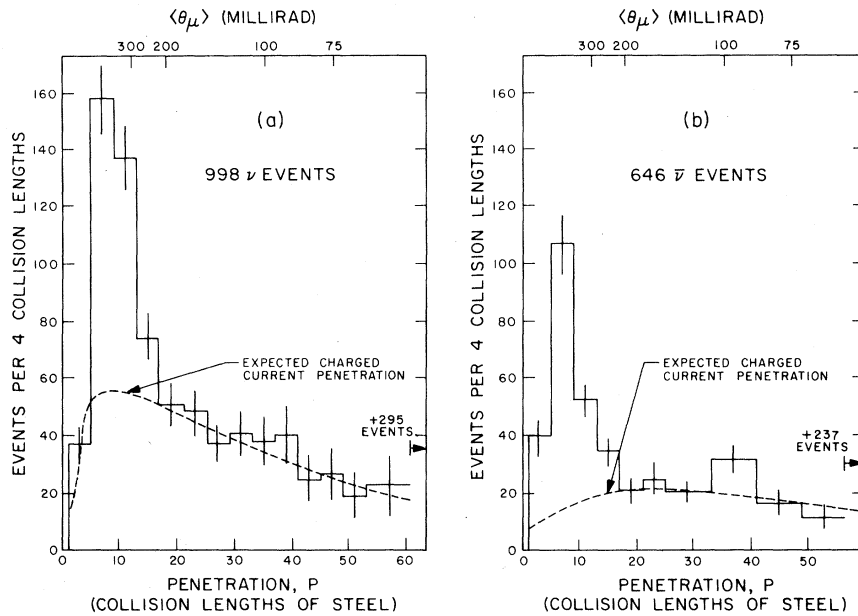


FIG. 1. Penetration distributions of events with no particles exiting through the end of the apparatus for (a) ν , and (b) $\bar{\nu}$. The smooth curves show the expected shape from CC events alone (wide-band contribution is included). The typical CC muon angle is shown on the top scale.

The existence of a muon in the final state is characterized by the presence of a very penetrating particle. To distinguish events with or without muons we determined for each event the number of collision lengths traversed by the *most penetrating* charged particle observed in the interaction. This penetration P was measured by the scintillation counters spaced every collision length. NC events are expected to have penetrations characteristic of their hadron-shower range (a 30-GeV proton produces a shower of average range $P = 11$ CL). For CC events, on the other hand, P is usually the longitudinal distance traveled by the muon before it stops or leaves the apparatus. Muons with small production angle θ_μ have the longest penetration.

Figures 1(a) and 1(b) show the experimental distributions in penetration for ν and $\bar{\nu}$ events, respectively, where the distributions have been corrected for the finite length of the detector.⁵ The smooth curves, normalized to all events with $P \geq 14$, represent the distributions expected from CC events alone. The excess of the data over the curve in the large peaks centered at $P \approx 9$ is indicative of a possible neutral-current signal. Possible backgrounds to such a peak are (a) cosmic-ray events, (b) ν_e events, (c) neutron interactions, and (d) CC interactions without identifiable muons. These will be considered in turn.

The first three of these were small. Cosmic-ray backgrounds were 2.1% of all $\bar{\nu}$ events and 0.3% of ν events as a result of the use of the fast-spill extraction and the 6-GeV cut in E_{had} . They were continuously monitored during the run in a separate "off beam" gate and have already been subtracted from all distributions shown. The electron-neutrino contamination in the beam has been calculated to contribute less than 3% of all ν events and less than 1% of all $\bar{\nu}$ events. The number of background events from neutrons would occur with characteristic attenuation of about 2 CL from the point of entry into the steel. Figure 2(a) shows no attenuation for NC candidates ($P \leq 13$) over a longitudinal distance of 50 CL from the front of the apparatus and Fig. 2(b) shows similar behavior over transverse distances of ± 6 CL. Appreciable background from any strongly interacting particle is thus ruled out.

The largest known background source is CC events with small penetration, as indicated by the extrapolated curves in Figs. 1(a) and 1(b). The curves were calculated by using the usual form of the differential cross section (consistent with previous analysis of CC data).⁶ The shapes of the curves for $P \leq 13$ are insensitive to deviations from this form.⁷

In order for CC events to produce a peak at small penetration (and thus at large muon angle)

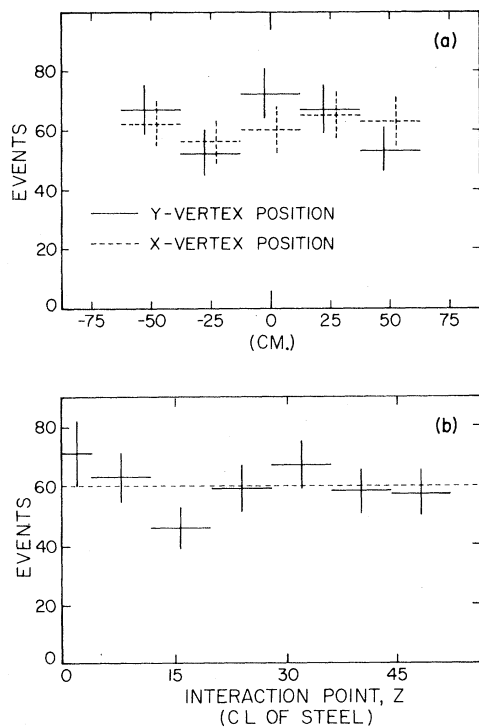


FIG. 2. Position in target of interaction vertex (ν events with $P \leq 13$ CL). (a) Transverse coordinates. (b) Longitudinal (z) coordinate.

there would have to be a perverse anomaly in the θ_μ distribution. The following argument shows that this hypothesis is not consistent with the data. Conservation of energy and momentum requires that wide-angle muons must have low energy; as θ_μ becomes large, $E_{\text{had}} \rightarrow E_\nu$. This behavior is illustrated in Fig. 3(b) by CC neutrino events with moderate penetration ($18 \leq P \leq 26$), corresponding to a typical muon angle of about 175 mrad. The experimental distribution peaks at $E_{\text{had}} = 20$ GeV, in agreement with calculation. The CC events with smaller penetration (and larger angle) will have even larger E_{had} , as shown by the calculated smooth curve in Fig. 3(c). However, the hadron energy distribution of events with $P \leq 13$ is similar to that of the CC data shown in Fig. 3(a).

The large number of low-penetration events cannot be attributed to low-energy muons from CC events unless there is an excessive number of low-energy beam neutrinos. The only such component comes from decays before the secondary hadron beam is momentum selected. This has been directly measured by closing the momentum-defining collimator. The number of CC

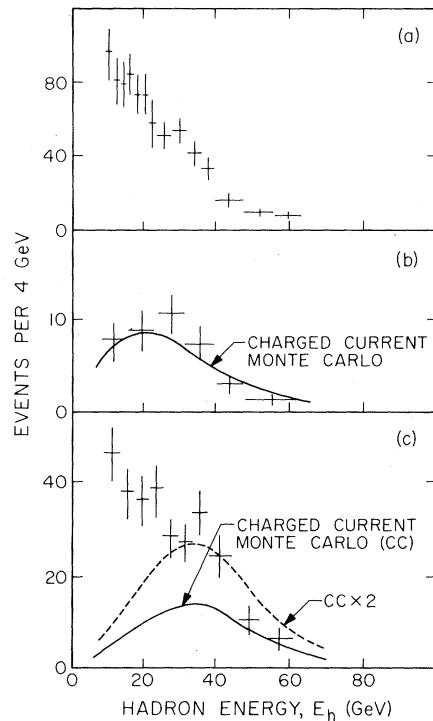


FIG. 3. Hadron energy for 998 ν events. (a) CC events with $P \geq 14$ CL (b) Intermediate-angle CC events ($18 \leq P < 26$ CL). (c) NC candidates ($P \leq 13$ CL). The smooth curves in (b) and (c) are expected distributions for CC events alone.

events from this source is $\leq 8\%$ of the events with small penetration shown in Fig. 3(c). Therefore, the shape of this distribution cannot be explained by wide-angle muons in the data. *In fact, this figure dramatically illustrates that a substantial fraction of events with $P \leq 13$ have unobserved energy transported out of the steel apparatus without interaction.* This implies that particles with strong or electromagnetic interactions are not carriers of the energy.

We conclude that events with no muon and with missing energy in the final state (consistent with the neutral-current hypothesis) are present for both neutrino and antineutrino interactions. After subtracting the CC background, the raw ratios of the excess events to ordinary CC events are $R_{\text{raw}}^\nu = 0.22$ and $R_{\text{raw}}^{\bar{\nu}} = 0.33$. We expect that the actual magnitudes of the effect are within a factor of 2 of these uncorrected values.

The most important correction involves the extrapolation to low hadron energy ($E_{\text{had}} \leq 6$ GeV), where the trigger has not reached full efficiency and event identification becomes difficult. If the

observed effect is due to neutral currents, the distributions in inelasticity $y = E_{\text{had}}/E_\nu$ depend on the type of coupling to the weak current.⁸ For example, the familiar $V-A$ neutrino interaction has constant dN/dy , but a scalar or pseudoscalar coupling would produce a distribution $dN/dy \propto y^2$, while a $V+A$ coupling would produce $dN/dy \propto (1-y)^2$. These different distributions reflect themselves in the E_{had} distributions. The $E_{\text{had}} > 6$ -GeV cut in the data gives detection efficiencies differing by almost a factor of 2 depending on which coupling is assumed. More detailed knowledge of the distribution in hadron energy will be necessary to determine the coupling mechanism and also to determine accurately the magnitudes of the ratios to ordinary charged currents.

*Work supported in part by the U. S. Atomic Energy Commission. Prepared under Contract No. AT(11-1)-68 for the San Francisco Operations Office, U. S. Atomic Energy Commission.

†On leave of absence from Ecole Polytechnique, Paris, France.

‡Swiss National Fund for Scientific Research Fellow.

¹S. Weinberg, Phys. Rev. Lett. **19**, 1264 (1967), and **27**, 1683 (1972); A. Salam and J. C. Ward, Phys. Lett. **13**, 168 (1964).

²F. J. Hasert *et al.*, Phys. Lett. **46B**, 138 (1973); A. Benvenuti *et al.*, Phys. Rev. Lett. **32**, 800 (1974); B. Aubert *et al.*, Phys. Rev. Lett. **32**, 1454, 1457 (1974); S. J. Barish *et al.*, Phys. Rev. Lett. **33**, 448 (1974).

³B. C. Barish *et al.*, NAL proposal No. E-21, 1970 (unpublished); P. Limon *et al.*, Nucl. Instrum. Methods **116**, 317 (1974).

⁴B. C. Barish *et al.*, Nucl. Instrum. Methods **116**, 4 (1974).

⁵Events which had charged particles leaving the detector through the downstream end are not included. The available fiducial volume for a particle of penetration P varies with P , becoming small when P approaches the length of the detector. The data have been corrected for this purely geometrical effect so that the resulting distribution is that of an infinitely long detector.

⁶B. C. Barish *et al.*, in Proceedings of the Seventeenth International Conference on High Energy Physics, London, 1-10 July 1974 (to be published).

⁷In particular, deviations from this form have been reported for $x \leq 0.1$ [B. Aubert *et al.*, Phys. Rev. Lett. **33**, 984 (1974)]. Such an effect would alter the curve primarily in the region of small θ_μ and large P , not in the small- P region.

⁸B. Kayser *et al.*, Phys. Lett. **52B**, 385 (1974).

SU(4) Explanation of the Narrow Resonances in e^+e^- Annihilation*

D. H. Boal, R. H. Graham, J. W. Moffat, and P. J. O'Donnell
Department of Physics, University of Toronto, Toronto, Ontario, Canada
 (Received 9 December 1974)

The narrow resonances at $M_\psi = 3.105$ GeV and $M_{\psi'} = 3.695$ GeV are assigned, together with the familiar SU(3) nonet of vector mesons, as members of the $1 \oplus 15$ representation of SU(4). This leads to a solution consistent with the observed particle spectrum and accounts for the narrow-widths of the ψ and ψ' . The masses of the charmed vector and pseudoscalar mesons are predicted.

A narrow resonance, ψ , at a mass of 3.105 GeV with a width $\Gamma_\psi \leq 1.3$ MeV was reported recently by the Stanford Linear Accelerator Center,¹ Brookhaven National Laboratory,² and Frascati³ groups. A second narrow resonance, ψ' , with a mass of 3.695 GeV has also been observed by the Stanford Linear Accelerator Center group.⁴

The narrowness of these resonances suggests that new selection rules are operating and that we have to consider higher symmetry groups such as SU(4) and SU(8).⁵ In the following, we shall investigate the consequences of assigning the ψ and ψ' to the $1 \oplus 15$ representation of SU(4).

To accommodate the ψ and ψ' in SU(4), we as-

sume that there exists a new semistrong interaction⁶ which breaks hypercharge and the new quantum number $W = \frac{1}{3}X - \frac{1}{4}N$ such that the total charge and isospin in the extended Gell-Mann-Nishijima formula⁷

$$Q = I_3 + \frac{1}{2}Y + \frac{1}{3}X - \frac{1}{4}N \quad (1)$$

are conserved. This interaction allows the single production of charmed particles as well as their decay into noncharmed ($W=0$) particles. We suppose that the ψ' is almost pure $|c\bar{c}\rangle$, while the ψ is almost entirely $|s\bar{c}\rangle + |c\bar{s}\rangle$. The new semistrong interaction causes mixing between these latter states and those with $Y=0$ and $I=0$ (i.e.,